Key Points:
- Hypsometric curves in combination with normalized terrain data can be used to assess soil moisture with limited data requirements
- The inclusion of flexible and scalable parameters facilitates local adaptation and allow a broad application of the proposed approach
- The proposed approach could prove useful for water balance calculations, flood management and agriculture

Correspondence to:
A. Bjerkén,
august.bjerken@tvrl.lth.se

Assessing Surface Saturation and Transpiration Potential by Hypsometric Curves and the HAND Model

August Bjerkén[1], Luz A. Cuartas[1,2], Luk Peeters[3], and Kenneth M. Persson[1]

[1]Division of Water Resources Engineering, Lund University, Lund, Sweden, [2]CEMADEN, São José dos Campos, Brazil, [3]Commonwealth Scientific and Industrial Organisation (CSIRO), Adelaide, SA, Australia

Abstract Methods for soil water conditions assessment are often highly localized or data demanding. In this study we propose a new scalable approach to assess soil water conditions. The main goal is to test whether the approach can be used to provide information about local conditions, without the need of extensive data sets. The approach utilizes a combination of normalized topography derived from the HAND terrain model (Height Above the Nearest Drainage) and hypsometric curves to identify wet and saturated areas for any given geographical extent. The study was conducted through a case study in the Lagan River catchment in the southwest of Sweden. To analyze the performance of the approach, a non-linear regression analysis was performed to assess the relationship between the fraction of wet area and the normalized terrain. This was followed by a correlation analysis, in which the correspondence of the derived output was validated against the national Soil Moisture Map provided by the Swedish University of Agricultural Sciences. The results show a strong, and statistically significant, negative exponential relationship between the fraction of wet area, and the maximum heights within the studied area. The approach also corresponds well with the spatial variations highlighted in the Soil Moisture Map, although better in predicted wetter areas than under dry conditions. Going forward, we believe the integration of hypsometric curves and the HAND model could not only improve water balance calculations but assist in the assessments of flood and drought-prone areas.

1. Introduction

Soil moisture is a term used to describe the water found within the rooting zone of vegetation (Legantes et al., 2011). Soil moisture plays an important role in the overall assessment of water availability, with runoff, infiltration, and discharge rates intricately linked to the soil water content of the rooting zone (Western et al., 2002). Furthermore, soil moisture is also important in agriculture and for the biodiversity of the landscape, as both plants and microbes rely on the availability of water within the soil (Dobriyal et al., 2012; Wall & Virginia, 1999). As such, understanding the importance of, and assessing, soil moisture is pivotal in the management of water resources (Dorigo et al., 2017). Despite this, soil moisture is often overlooked when assessing the whereabouts and total potential water storage within the landscape (Liu et al., 2017). However, as the effects of human-induced climate change are starting to become more and more obvious, with changed precipitation patterns and increased periods of extreme weather we see that many places, both previously affected and unaffected, are starting to experience the effects of water scarcity (Zhou et al., 2021). As a result, research concerning the interaction between surface- and groundwater, including soil moisture mapping, has seen a resurgence in recent years (Condon et al., 2020; Taylor et al., 2013; Wu et al., 2020).

There are several approaches to assessing soil water content, including contact-based field measurements and contact-free approaches such as ground penetrating radar (Huisman et al., 2003; Kaufmann et al., 2020; Klotzsche et al., 2018), remote sensing (Babaeian et al., 2021; Capehart & Carlson, 1997; Neale et al., 2012), data assimilation (Heathman et al., 2003; Renzullo et al., 2014), wetness index (Barling et al., 1994; Brocca et al., 2010), and neural networks (Chaney et al., 2015; Yuan et al., 2020). Despite this, most approaches have a limited scaling ability (Brocca et al., 2012; Korres et al., 2015; Western & Blöschl, 1999). This can make it difficult to find a good fit, especially when working on catchment-wide assessments where the relative importance of adjusting for local variabilities can vary (Teuling & Troch, 2005; Western et al., 2004). In addition, catchment-wide assessments of soil saturation are generally not only costly, but complex endeavours that require great knowledge of the studied area (Bittelli, 2011; Rosenbaum et al., 2012). While the inclusion of detailed information regarding local conditions allows researchers and managers to get an in-depth understanding of soil saturation, the high data requirements heavily limit the application of many approaches (Bolten & Crow, 2012;
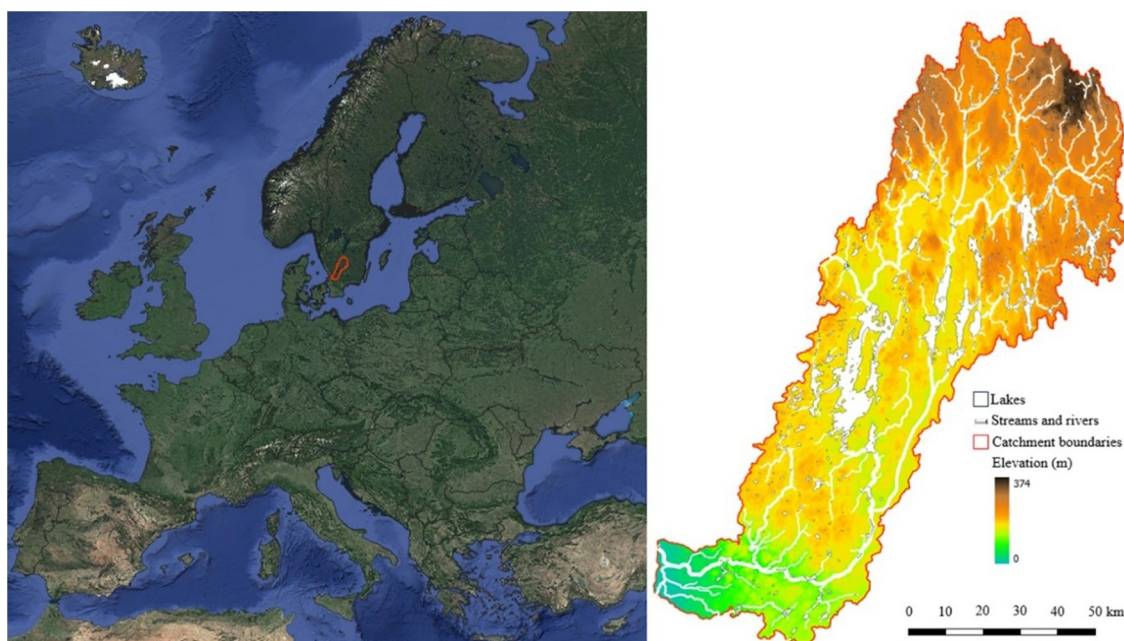
Figure 1. Location of the Lagan River catchment in southwestern Sweden showing the overall elevation and the presence of lakes and water courses within the catchment.

Yuan et al., 2020). This is especially true in areas where access to historical data used for calibration and validation is poor and data collection is made difficult (Rödiger et al., 2014).

In this paper, we describe a new approach for assessing surface saturation and transpiration potential within catchments. The approach, consisting of a combination of an existing HAND (Height About the Nearest Drainage) normalized terrain model (Nobre et al., 2011) and information regarding the cumulative distribution of elevation, is the first approach in which information about a catchment's topography is the basis of the entire assessment. By removing the large sets of spatial data and local adaptations required when assessing soil moisture conditions, the suggested approach provides researchers and managers with a quick, scalable and cost-efficient way to assess the general conditions of a catchment, regardless of the catchment's size. To test and verify the suggested approach, a case study was carried out in the Lagan River catchment in Sweden. There, the fraction of drainage networks, f_D, wet areas, f_W, saturation at the surface, f_{sat}, and the area accessible for transpiration from groundwater, f_{Eg}, was determined for 325 individual hydrological response units (HRUs) of 25 km^2 within the catchment.

2. Materials and Methods

2.1. Study Area

The Lagan River catchment is located in the southwest of Sweden (56°47' to 57°23' N latitude and 13°53' to 14°31' E longitude, Figure 1) with a drainage area of 6,445 km^2. The elevation ranges from 0 to 374 m above mean sea level, with the highest points found in the northern parts of the catchment. The climate is classified as a warm-summer humid continental climate according to the Köppen-Geiger classification (Beck et al., 2018), with an annual average precipitation of 675–900 mm (Klante et al., 2021). The predominant land cover in the catchment is mixed coniferous forest, except for the southwestern section where agricultural land-use dominates. The major economic activities include forestry, agriculture, hydroelectric power generation, as well as light- and heavy industry. The soil is dominated by till, except for the southwestern fluvial plains where post-glacial sand and silt make up a large proportion. Glaciofluvial deposits can also be found at several locations within the catchment, with notable concentrations around River Lagan.

From a water resources perspective, the catchment comprises 511 lakes and 97 aquifers, with a combined maximum storage capacity of 9.36 km^3 (Bjerkén & Persson, 2021). Of this, aquifers make up 7.10 km^3, the majority of which are situated in the large glaciofluvial deposits in close connection to the river Lagan. Looking at
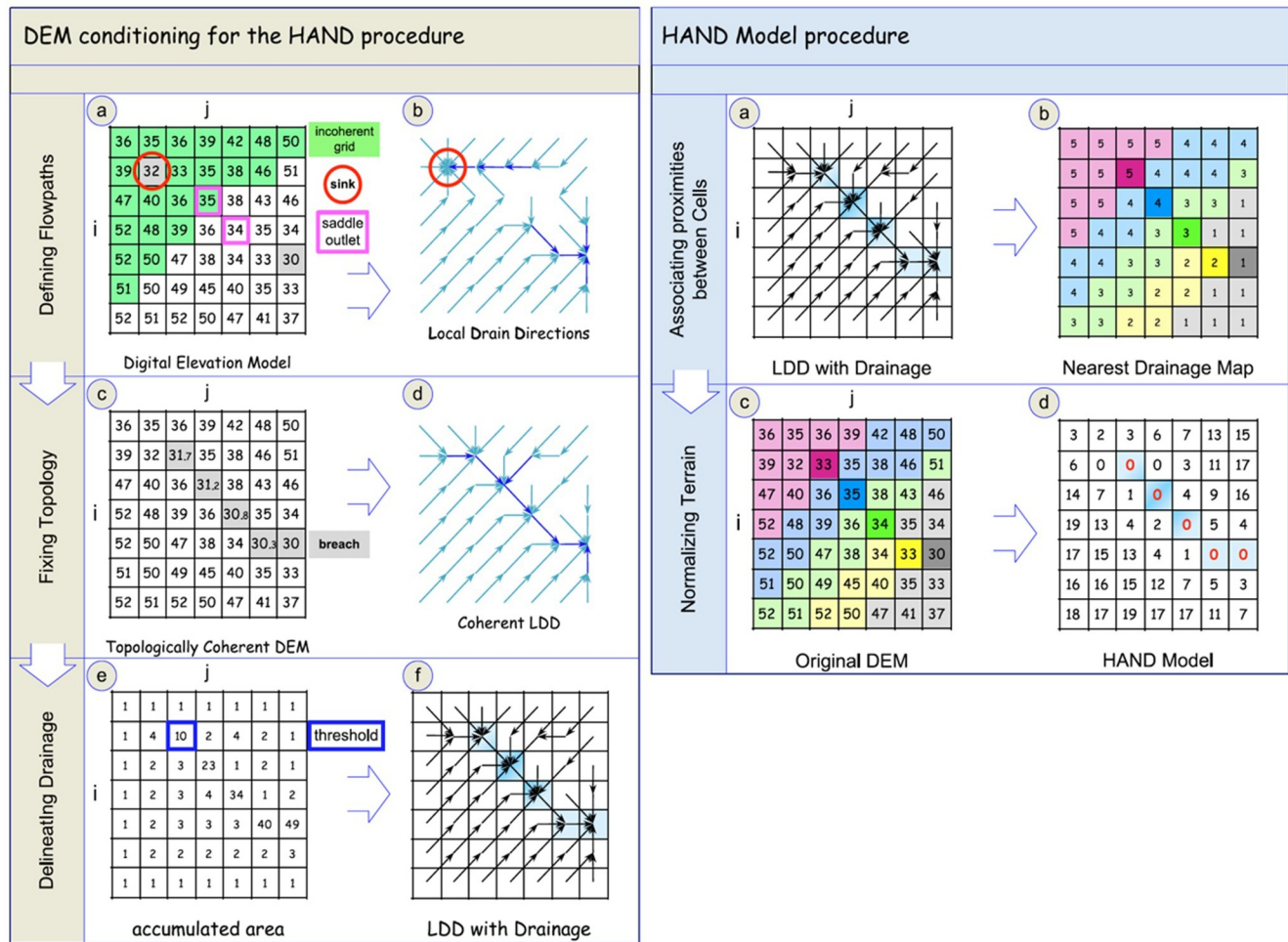
Figure 2. Conceptual structure of the HAND model (diagram adapted from Nobre et al., 2011).

the remaining 2.26 km³ attributed to lakes, more than 40% (0.97 km³) can be found in Lake Bolmen. Located in the central part of the catchment, west of River Lagan, Lake Bolmen is Sweden's twelfth largest lake and the main drinking water source for more than 500,000 people (Sydvatten, 2015). Given the importance of the catchment from drinking water perspective, increased understanding of the available water and storage potentials is crucial not only to improve the accuracy of water balance calculations within the catchment but in the long-term sustainable management of the water resources within the region.

2.2. HAND Model

Height above nearest drainage (HAND) is a terrain model built around the normalization of topography (Figure 2). First developed by Nobre et al. (2011), the HAND model offers a novel and unique ability to study and classify the topographic relation between soil and water (Nobre et al., 2011). The HAND model can be divided into four steps: fixing topology (hydrological coherent topography) and defining flow paths, delineating drainage, associating digital elevation model cells with the cells of the nearest drainage, and normalizing the terrain.

2.2.1. Procedure

The first step consists of fixing the topology and defining existing flow paths in a digital elevation model (DEM). Sinks and saddle outlets are then identified, allowing the analyzed area to be divided into two or more incoherent pixels, given there exists any saddle outlets. The local drain direction (LDD) is then derived for all pixels. Next, depression breaching is applied to the identified sinks within the original DEM-raster subsequently removing any potential saddle outlets. This creates a topologically coherent DEM, which in turn allows for the topological

Table 1
HAND Terrain Classes as Identified by Nobre et al. (2011)

	HAND terrain class	Description	Definition
	Waterlogged	Saturated lowland	$0 \leq$ HAND ≤ 5 m above the nearest drainage
	Ecotone	Unsaturated lowland	$5 \leq$ HAND ≤ 15 m above the nearest drainage
	Sloped	Upland with higher slope angles	>15 m above the nearest drainage and $\geq 7.6\%$ slope
	Plateau	Upland with lower slope angels	>15 m above the nearest drainage and $<7.6\%$ slope

Note. Colors are derived from the plotting of the HAND-model as shown in Figure 6.

correction of the previously defined LDD. In the second step, delineating drainage, the total area that drains into each cell is first calculated based on the direction of the downhill flow (flow paths), subsequently creating an accumulated area grid. Next, an accumulated area threshold value is determined for the stream origins, thereby defining the drainage network. In the third step, associating digital elevation model cells with the cells of the nearest drainage, a nearest drainage map is calculated using the flow paths to connect all cells (pixels) with the cells of the nearest drainage. In the fourth and final step, normalization of terrain, the elevation difference between each grid cell and its nearest drainage point (connected throughout the flow paths) is calculated. This normalizes the terrain, while at the same time ensuring that the model, rather than having to refer to the height above sea level, refers to the height above the nearest drainage.

2.2.2. HAND Terrain Classes

In order to assess the hydrological relevance of the normalized terrain, and to facilitate the visualization of changes to the soil environment throughout the terrain, Nobre et al. (2011) identified a number of HAND terrain classes. Table 1 shows the HAND terrain classes included in the model. These include two lowland classes: waterlogged and ecotone, as well as two upland classes: slope and plateau. Waterlogged terrain are saturated lowland areas that are characterized by a high-water table or frequent water inundation (Nobre et al., 2016). Predominantly found within close proximity to water bodies and naturally occurring topographic sinks, water-logged terrain is defined as any area within 5 m elevation from the nearest drainage breach. Ecotone terrain is used to describe the unsaturated lowland with shallow water table located 5–15 m elevation from the nearest drainage breach. Often found in areas within the transition zone between lowland and upland regions, ecotone terrain is similar to waterlogged terrain defined based on the range of heights. Sloped terrain is defined as areas with a slope angle of more than 7.6% and an elevation of more than 15 m above the nearest drainage point. Often found in areas with a sharp incline or decline such as on the sides of hills or mountains, sloped terrain is generally well drained, with a relatively deep-water table. This is also true for the second upland class, plateau. However, unlike the sloped terrain, plateaus occur in areas where the slope angle is less than 7.6%.

As explained in Nobre et al. (2011) the gravitational potential is a physical force that affects any liquid on and in the terrain, causing it to move downward. As a result, water either percolates into the porous media (if not saturated) or flows downhill as runoff, ultimately draining to the stream. The HAND model equates a relative gravitational potential to a draining potential, which measures the net ability of water to drain from its position on the hillslope to the nearest drainage. Higher HAND heights imply a larger draining potential, leading to the appearance of a vadose zone where water will drain effectively. On the other hand, lower HAND heights mean low draining potential and proximity to the water table, where draining water will pool, creating waterlogging. The correlation of terrain types with distinctive HAND height classes demonstrates a significant correlation with soil-water saturation. The depth of the saturated zone determines the superficial soil-water environment.

Nobre et al. (2011) also demonstrated that soil type or slope do not interfere in the HAND class transition, because soil water movement along flow paths toward the stream is propelled solely by relative gravitational potential, or drainage potential. And it turns out that 5 m unlevel for the first class (waterlogged) and 15 m for the second class (ecotone) has strong and consistent correlation with water table depth regimen. 5 m HAND unlevel to the nearest stream, or smaller, delineates terrain with superficial or near superficial water table. Between 5 and 15 m HAND the unlevel water table starts to get away from the surface but is still reachable by plant roots. Above 15 m HAND unlevel are terrains with a significant vadose zone. Because the HAND model describes a physical property of the
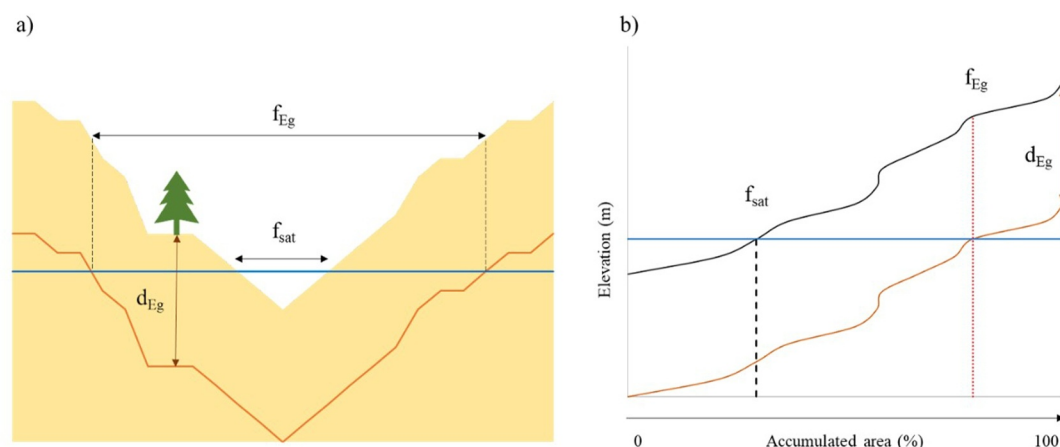
Figure 3. Conceptual relationship between groundwater storage, the fraction of saturation, f_{sat}, and the fraction accessible for transpiration, f_{Eg}. d_{Eg} is used to describe the maximum root depth, given in meters. (a) Subsurface conceptualization (b) Hypsometric curve showing the cumulative distribution of elevation for the area described in panel (a).

landscape, the topology of local drainage potentials, it is independent from soil type, geology, geomorphology, or climate.

2.3. Hypsometric Curves

Introduced by the American hydrologist Walter B. Langbein, and later developed by Arthur N. Strahler, hypsometric curves are used to describe the cumulative distribution of specific elevations within an area (Langbein, 1947; Strahler, 1952). By assessing the area-elevation distribution, Langbein and Strahler showed that it is possible to not only express the slope of a catchment using topographical data but also identify relief rate and drainage areas within the catchment (Vivoni et al., 2008).

Peeters et al. (2013), assuming a topography-controlled and uniform distribution of groundwater storage, a flat-water table, and a fixed root depth, assessed the fraction of saturation and fraction accessible for transpiration, using hypsometric curves. Figure 3 shows the conceptual relationship between groundwater storage, the fraction of saturation, f_{sat}, and the fraction accessible for transpiration, f_{Eg}, as described by Peeters et al. (2011). First, the cumulative distribution of the elevation (black) and responding root depth (brown) is plotted using hypsometric curves, see Figure 3. Next the water table is added (blue). Once plotted, the fraction of the area located below the water table is then calculated for both hypsometric curves.

2.4. Setup

2.4.1. Structure

In Figure 4, the conceptual structure of the proposed approach is demonstrated. The approach consists of three main steps, with an additional two optional steps. In the first step, elevation data and geospatial data pertaining to the delineation of catchment boundaries are imported. In case spatial delineation is required, the catchment is divided into a number of hydrological response units (HRUs) using a 5 × 5 km grid. Next, elevation data for each of the HRUs is normalized using the 0.5.1 Alpha version of the HAND-model, as described in Section 2.2. The normalized output is then converted from raster files to .csv files using QGIS v.3.28.9. Next, the maximum root depth (d_{Eg}) is set. For the general approach, d_{Eg} is set to 7 m, based on the maximum root depth of tree on a global scale as defined by Canadell et al. (1996). In case the user prefers to use other values to get a more detailed understanding of the fraction of groundwater accessible to a specific species, this value can be modified.

Once a threshold value for the maximum root depth has been set, the cumulative distribution of the normalized elevation is then plotted for each HRU using hypsometric curves. Based on the accumulated area where the height above the nearest drainage point is equal to 0 m, the fraction of each HRU made up by drainage networks, f_D is determined using:
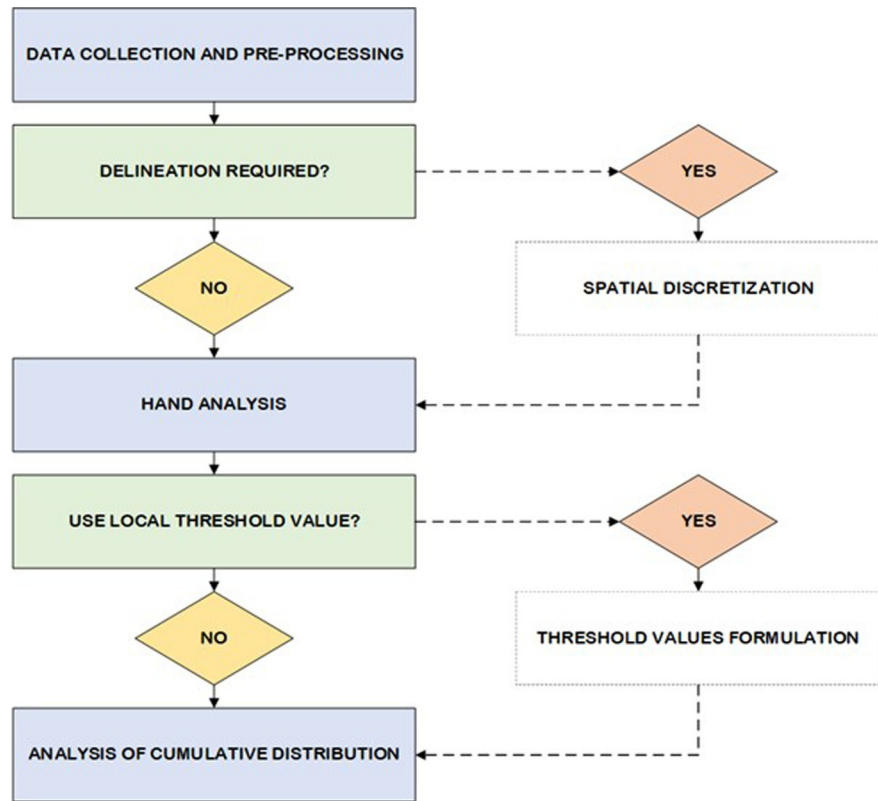
Figure 4. Conceptual structure of the proposed approach. The blue boxes represent required steps, and the green boxes optional steps. The dotted boxes represent additional steps involving further data processing.

$$f_D = \frac{A_D}{A_{tot}} \tag{1}$$

where A_D is the accumulated area at drainage level, and A_{tot} is the total area of the HRU.

Next, the fraction of wet area, f_W, is determined for each HRU using:

$$f_W = \frac{A_W}{A_{tot}} \tag{2}$$

where A_W is the accumulated area within 5 m elevation above the nearest drainage point.

Next, the fraction of saturation, f_{sat}, is determined for each HRU using:

$$f_{sat} = \min\left(\frac{A_{tot} - A_D}{A_{tot}}, \frac{A_W - A_D}{A_{tot}}\right) \tag{3}$$

The fraction of saturation, f_{sat}, corresponds to the area of the HRU that is found within 5 m elevation of the nearest drainage point minus the area found at drainage level.

Lastly, the fraction of the HRU that is within an elevation where transpiration from groundwater can take place, f_{Eg}, is then determined using:

$$f_{Eg} = \min\left(\frac{A_{tot} - A_D}{A_{tot}}, \frac{A_{dEg} - A_D}{A_{tot}}\right) \tag{4}$$

where A_{dEG} is the accumulated area at or below the limit for maximum root depth.
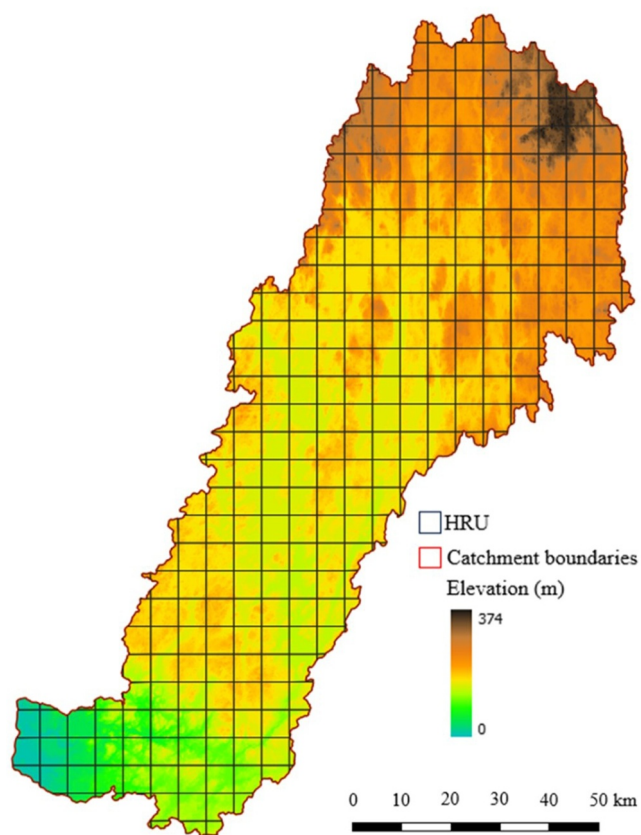
Figure 5. Map showing the Lagan River Catchment and the 325 HRUs used as outliers in the assessment of the catchment.

The fraction of the area where transpiration from groundwater can take place, f_{Eg}, corresponds to the area of the HRU that is found within the combined elevation of the water table (5 m) and the maximum root depth (7 m) minus the area found at drainage level. For the general approach, the elevation is set to (12 m).

2.4.2. Data

Elevation data was acquired from the NASA Shuttle Radar Topography Mission (SRTM) V3 Global 1 arc second data set, featuring a raster resolution of 30 m, and a spatial extent of (60.0°, 180.0°; −56.0°, −180.0°). Geospatial data pertaining to the delineation of catchment boundaries was obtained from Svenskt Vattenarkiv (SVAR), an openly accessible database administered by the Swedish Meteorological and Hydrological Institute (SMHI).

2.5. Validation

To assess the relationship between the fraction of wet areas, f_W, and the cumulative distribution of relative heights obtained from the HAND model, a non-linear regression analysis was conducted. The method was selected based on the perceived non-linear relationship between topography and the depth of the water table (Condon & Maxwell, 2015). First, the mean fraction of saturation, f_{sat}, was plotted against the cumulative distribution of relative heights for the included HRUs using a scatter plot. Next, an exponential model was fitted to the data, and the rate of decay and direction of the relationship was then determined. Next, the t-values and p-values were computed to assess the statistical significance of the studied relationship. Finally, the residual standard error (RSE) was determined and added to the plotted data.

To test the performance of the suggested approach, a spatial comparison was conducted against the SLU Soil moisture map (Ågren et al., 2021). First developed at the Department of Forest Ecology and Management, at the Swedish University of Agricultural Sciences (SLU), the SLU Soil moisture map is a high-resolution nationwide soil moisture map derived using a combination of LIDAR-derived terrain indices and machine learning. The map utilizes a scale from 0 to 100, where high values represent a high probability of the area being wet, and low values suggest a low probability. By comparing the fraction of wet area, f_w, derived using the suggested approach with the corresponding mean probability of wetness for each of the 325 hydrological response units, the performance of the suggested approach was assessed.

3. Results

3.1. Assessment

To allow for the assessment of the spatial variation of soil moisture within the catchment, a spatial discretization of the obtained DEM-file was performed. Figure 5 shows the spatial delineation of the studied catchment after applying a 5 × 5 km grid. Each "box" represents a hydrological response unit (HRU), ranging from 0.006 km^2 (HRU218) to 25 km^2. Of the 325 included HRUs, 41 have an area of <5 km^2, all of which can be found along the perimeter of the catchment.

Next, the distribution of heights above the nearest drainage was calculated for each of the 325 HRUs. In Figure 6, the distribution of heights above the nearest drainage is shown for one of the hydrological response units included in this study, HRU1. As can be seen in the figure, a large part of the area has a height above the nearest drainage of less than a few meters, with only limited peaks present. This, combined with the area's geographical location at the bottom of the drainage basin, and the area's relatively low elevation, as shown in Figure 5, suggests that large parts of the area are either fully, or partly, saturated.

Finally, the cumulative distribution, or accumulated area, was calculated for each of the 325 HRUs based on the HAND model output. Figure 7 shows the cumulative distribution of heights above the nearest drainage depicted in
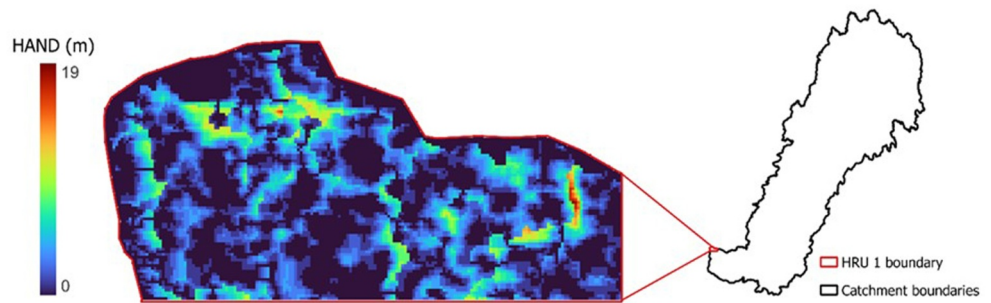
Figure 6. Map showing the difference in height above the nearest drainage cell for one of the HRUs (HRU1) included in the study. The blue areas are considered wet.

Figure 6. As suggested by the initial HAND analysis, a large proportion of the area can be found within only a few meters of the nearest drainage, with a total of 85.4% of the area deemed to be wet terrain. Of this, 36.2% of the HRU is made up by drainage networks, and 49.2% by areas saturated at the surface. Looking at the fraction of the HRU available for transpiration to take place 97.9% of the HRU is deemed to be within the limit 12 m elevation above the nearest drainage, with a total of 61.7% deemed to be made up by areas accessible for transpiration from groundwater. This supports the claims made in the previous paragraph, that a large fraction of the area within the HRU is deemed accessible for transpiration.

3.2. Spatial Distribution

Figure 8 shows the spatial distribution of the maximum heights above the nearest drainage cell within each of the 325 HRUs studied within the Lagan River catchment. HRUs with maximum HAND heights were found in areas located close to the edges of the catchment, and in areas where natural ridges occur. This was especially prevalent in the highlands of the catchment, and in the sloped areas found in the southwest corner of the catchment. Lower ranges were predominantly found in HRUs within the low-lying areas near the outlet of the catchment, and those dominated by open surface water bodies. In addition, lower distribution was also found in several of the smaller HRUs located at the edges of the catchment where the total pixel count was that of 20,000 or less.
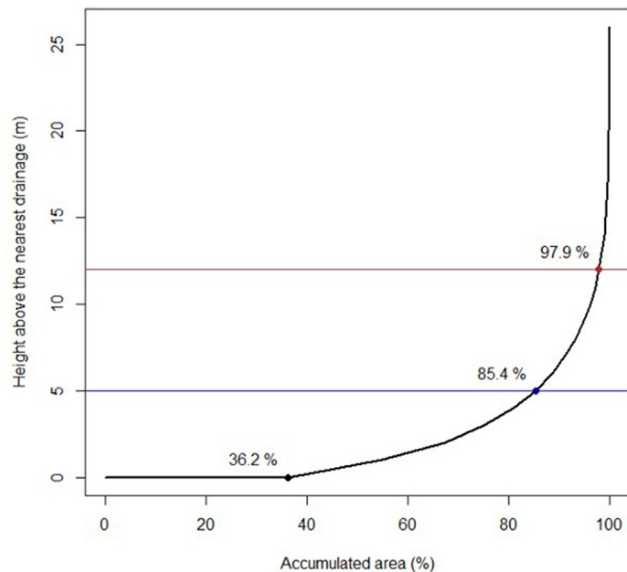
Based on the assumption of a topography-controlled and uniform distribution of groundwater storage, a flat-water table, and a fixed root depth, the fraction of drainage networks, f_D, wet area, f_W, saturated area, f_{sat}, and the area accessible for transpiration from groundwater, f_{Eg}, was determined for all 325 HRUs. Figure 9 shows the spatial distribution of the different fractions in the catchment. Looking at the fraction of drainage networks the highest values were found HRUs dominated by, or in close proximity to, open surface water bodies. Similarly, the fraction of wet areas were also high in these areas. However, high fractions of wet area were also found in areas with a low range of the maximum heights above the nearest drainage. In these areas, the fraction of saturation and fraction of the HRU accessible for transpiration from groundwater were also found to be on the higher end. In HRUs with a high fraction of the total area made up by drainage networks, f_{sat} and f_{Eg} were found to be toward the lower end. This suggests that in areas dominated by open water bodies, the fraction of saturated soils will be lower as more of the low-lying areas will be fully submerged.

3.3. Validation

3.3.1. Statistical Analysis

To evaluate the statistical significance of the suggested approach, a nonlinear regression analysis was performed. First, the fraction of wet area was plotted

Figure 7. Cumulative distribution over HRU1. The blue line shows the upper boundary for the wet terrain at 5 m above the nearest drainage. The red line shows the corresponding HAND value, 12 m, relative to a root depth of 7 m. The black marker shows the fraction of the accumulated area at the level of the drainage network. The blue marker shows the fraction of the HRU classified as wet areas. The red marker shows the fraction of the HRU located within the physical limits for root uptake to take place.
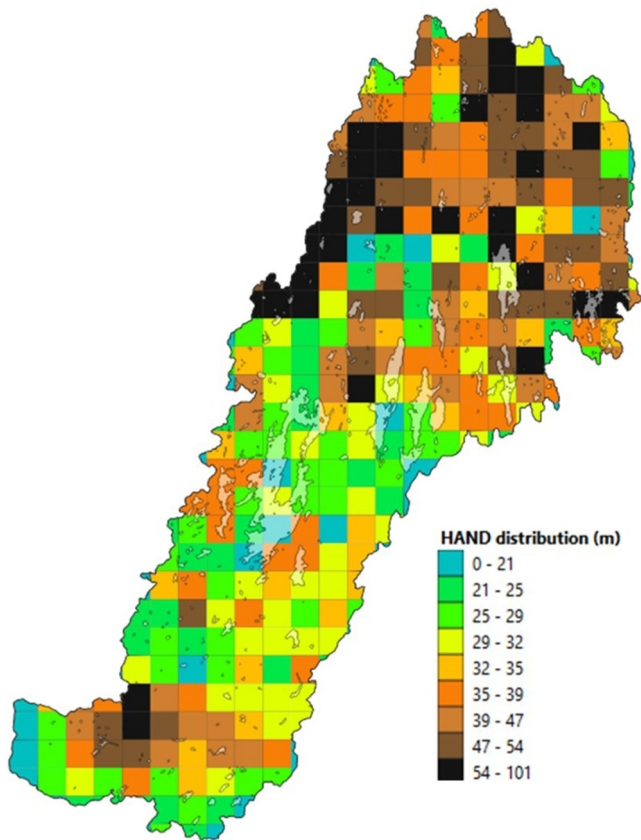
Figure 8. Map showing the spatial distribution of the maximum heights above the nearest drainage in each of the 325 individual HRUs defined within the Lagan River catchment.

against the cumulative distribution of relative heights for the 325 HRUs using a scatter plot. An exponential relationship of $y \sim a * \exp(b * x)$ was then fitted to the data. Figure 10 shows the non-linear relationship between the fraction of wet area and the cumulative distribution of relative heights obtained from the HAND analysis. The analysis shows a negative exponential relationship, with an exponential decay (b) of 0.0056681 and a p-value of 2e−16. This indicates a strong, and statistically significant, negative exponential relationship between the fraction of wet area, and the cumulative distribution of relative heights.

3.3.2. Spatial Analysis

Figure 11 shows the linear relationship between the fraction of wet area, f_W, and the mean probability of wet classification, P, derived from the soil moisture map provided by the Swedish University of Agricultural Sciences. In Figure 11a, the calculated values for all HRUs are included. The analysis shows a moderate positive correlation (0.49) between the calculated fraction of wet area and the predicted probability of wet classification, with a R^2 value of 0.24.

While the scatterplot shows that the HAND-hypsometric approach is prone to overestimating wetness, a strong linear tendency was detected for HRUs deemed to have a mean probability of wet classification of $P => 50\%$.

To test whether a stronger relationship could be found for HRUs with a mean probability of wet classification of $P => 50\%$, an additional correlation analysis was conducted for all HRUs within the P interval of 50%–100%, as seen in Figure 11b. The analysis shows a strong positive correlation (0.78) between the calculated fraction of wet area and the predicted probability of wet classification, with a R^2 value of 0.61. This suggests that in areas where the SLU Soil Moisture Map predicts a probability of wet classification at 50% or above, the proposed approach performs better than in predicted dryer areas.

4. Discussion

In the wake of the emergence of highly sensitive sensors and the development of computer-aided data processing software, the level of data available to soil moisture modelers has skyrocketed over the last few years, and with it, the complexity of the assessments (Johnston & Smakhtin, 2014). However, while the introduction of parameters such as porosity, land-use, and flow, on paper should increase the accuracy of the assessment, several studies have shown that the accuracy of soil moisture assessments in fact seldom relate to the complexity of the applied model (Brocca et al., 2010; Meng & Quiring, 2008; Vereecken et al., 2008). Instead, the accuracy of a model often boils down to how well the model fits within the local conditions, and the available data.

In this study we propose a scalable and cost-efficient approach to identify areas of interest from a soil water content perspective. We show that by applying an integrated approach combining the HAND model and hypsometric curves, it is possible to assess the soil moisture of any given area without the need of extensive amounts of data. The results from the non-linear regression analysis shows a strong negative exponential relationship between the fraction of wet area and the maximum heights above the nearest drainage within the studied HRU.

By comparing the derived values with the SLU Soil Moisture Map, we found a moderate correlation between the two models when comparing all the HRUs and a strong correlation in HRUs with a perceived probability of wetness of >50%. While the occurrence of a weaker correlation suggests that the proposed approach performs better in low-lying wet areas, the difficulties associated with the development of accurate assessment for sloped terrain solely based on information about the topography has long been discussed among the soil saturation modeling community (Condon & Maxwell, 2015; Gleeson et al., 2011; Haitjema & Mitchell-Bruker, 2005). While the water table to a great extent tends to mimic the topography of a catchment, the presence of topography-controlled water tables are more likely to occur in areas with a low hydraulic conductivity and flatter terrain
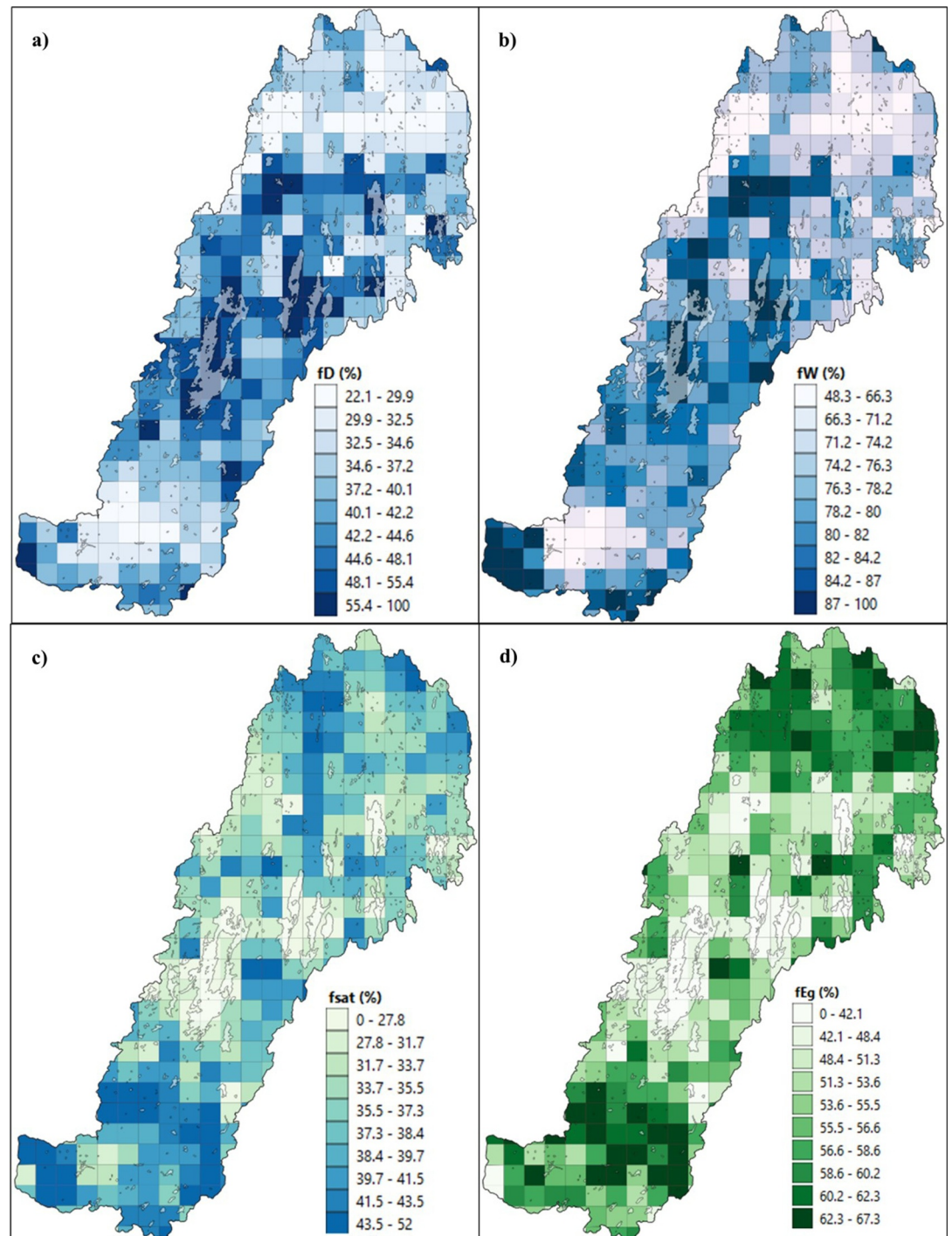
Figure 9. Map showing the spatial distribution of lakes throughout the catchment and the fraction of the HRU that is (a) comprised of drainage networks or water bodies, (b) wet areas, (c) saturated at the surface and (d) accessible for transpiration from groundwater in each of the 325 individual HRUs defined within the Lagan River catchment.

(Gleeson et al., 2011). As such, most topography-controlled approaches tend to perform better when assessed against wetter conditions, at least under the assumption of a topography-controlled water table (Grabs et al., 2009). However, looking at the strong correlation found between the proposed approach and the SLU Soil Moisture Map in the wetter areas of the study area, the results indicate that our approach performs at a similar level as the much more complex SLU model. This is especially true given the vast difference in the amount of data
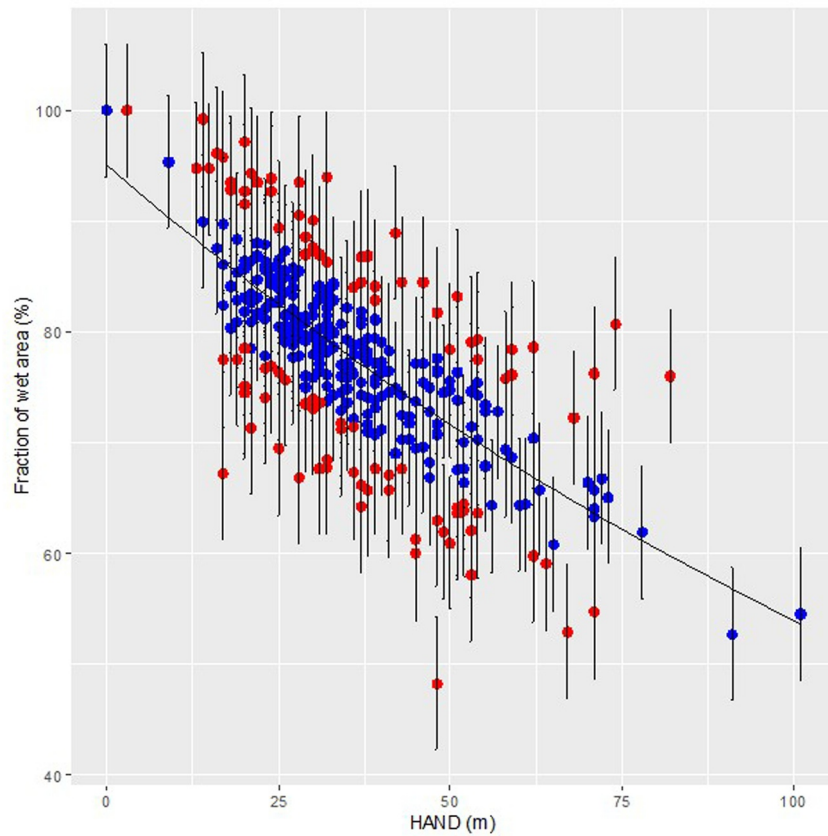
Figure 10. Scatter plot of the fraction of wet area and the range distribution of heights above the nearest drainage HAND derived from 325 HRUs along with the exponential fit of the model. The blue markers show values within the residual standard error (6.02) of the curve. The red markers show values outside of the residual standard error.

Figure 11. Scatter plot of the fraction of wet area, f_W, and the mean probability of wet classification, P, derived from the soil moisture map provided by the Swedish University of Agricultural Sciences. (a) Shows the relationship when including all 325 HRUs. The red box highlights the area where $P => 50\%$. (b) Shows the relationship when only including HRUs with a mean probability of wet classification of $P => 50\%$.

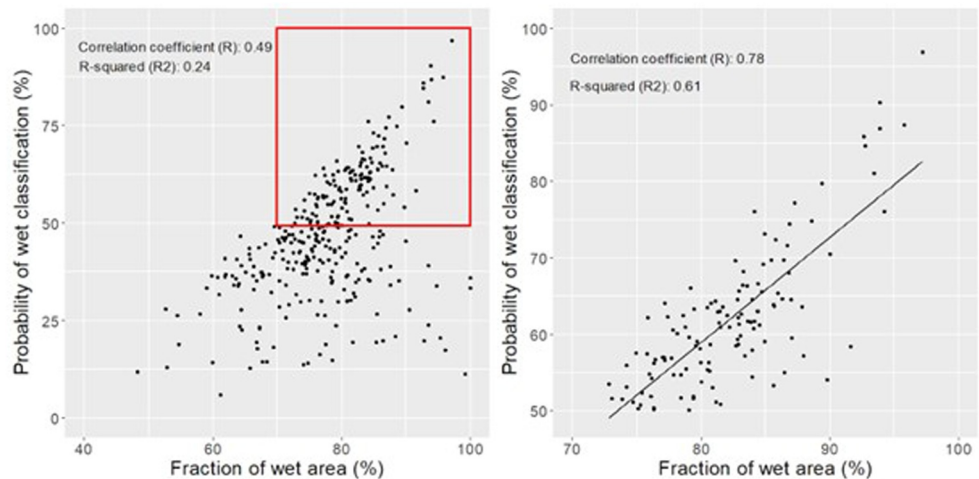required to operate the two different approaches, with the proposed approach relying on a single DEM-file in comparison to the combined information regarding 28 soil, climate, and environmental features, as well as the 19,643 field plots used to set up training data sets, required to construct the original SLU Soil Moisture Map.

Although the statistical analysis indicates that the suggested approach holds great promise, there are a number of challenges associated with the suggested approach that need to be addressed. These include the approach's limited temporal application, the underlying HAND model's high sensitivity to drainage channel network initiation thresholds, and scale issues. Starting off with the approach's limited temporal application, it is important to remember that as of today the approach does not include any temporal parameters. Instead, assessments are conducted solely based on spatial data input. As a result, users are provided with a snapshot of the local spatial conditions, which, while useful in the construction of a baseline for further assessments, makes it very difficult to assess any long-term changes to the soil water content. Moving forward, the underlying HAND model's high sensitivity to drainage channel network initiation thresholds pose another potential concern. As previously discussed by Gharari et al. (2011), this poses a problem, as the threshold directly influences the classification of the different terrain classes, as pictured in Table 1. However, as described by Nobre et al. (2011), the effect of slightly varying channel heads on the HAND model will not be significant if the calculated drainage network density remains within the range that captures the Strahler order of the real drainage network. As such, the sensitivity does not constitute a major concern, as long as the Strahler order is kept consistent throughout the assessment.

Looking at the three major challenges associated with the implementation of the suggested approach, scale issues constitute the most pressing concern. As with all land surface- and hydrological models, the implementation and output from the suggested approach greatly depend on the quality of the spatial data. This is particularly evident in mountainous areas, where the large topographic differences means that the resolution of the DEM file and the placement and delineation of the hydrological response units used in the assessment will have a high impact on the output of the overall assessment. In addition, modellers trying to apply the suggested approach within a mountainous area are faced with yet another challenge, as the sloped terrain means that it is difficult to assume a topography-controlled water table. As a result, it is difficult to properly assess and draw any results regarding the fraction of area saturated at the surface, f_{sat}, and the fraction that is accessible for transpiration from groundwater, f_{Eg}.

Despite these challenges, we believe that our findings can provide researchers and managers working within water resources management with a powerful, and cost-efficient tool to identify areas of interest from a soil water content perspective. One area of particular interest is the improvement of water balance calculations. By facilitating the process of obtaining detailed information regarding local soil moisture conditions, the accuracy and range of the water balance calculations can be improved (Alvarenga et al., 2017; Cuartas et al., 2012), as information about the water content of the soil is crucial to properly assess the rate of evapotranspiration that takes place (Evett et al., 2012). This is especially true in dryer areas, where the output from water balance calculations tend to be more sensitive to local soil conditions (Atkinson et al., 2002). Furthermore, the possibility to incorporate detailed information on the fraction of saturation could help to identify areas within a catchment suitable for increased storage (Tian et al., 2017). Beside the potential benefits associated with the improvement of water balance calculations, the integration of the HAND model in the proposed approach could also provide very useful input of value to a number of other applications, including the management of floods (Fang et al., 2023; Komolafe et al., 2020; Nobre et al., 2016; Scriven et al., 2021). The possibility to quickly assess the location of wet areas within a specific area or in a catchment, could help identify areas at risk of flooding, as shown by Nobre et al. (2016). While the ability to identify areas at risk has been included since the release of the HAND model, the possibility to analyze the cumulative distribution of elevations within an area through the use of hypsometric curves allows the user to quickly get an understanding of the size of the area at risk. Furthermore, the identification of dryer patches with a low soil water content could help in the management of forest fires (Keetch & Byram, 1968). While the causes of forest fires vary, studies have shown that the soil water content plays an important role in not only controlling the spread and magnitude of forest fires, but the length of the fire season (Bartsch et al., 2009; Rakhmatulina et al., 2021). Finally, the suggested approach offers promising applications in the agricultural domain. By providing researchers and managers with an efficient tool to evaluate local topographical conditions, without the use of extensive data set or local knowledge, the suggested approach enables swift and cost-effective identification of suitable cultivation areas for specific crops (Hashemian et al., 2015). This is further supported by the users' ability to freely adjust the threshold value for root depth when assessing the fraction of the area where transpiration from groundwater can take place, f_{Eg} (Durrant et al., 1973). While a better

understanding of local soil moisture conditions not only allows farmers to make a more informed decision about which crop to cultivate, the information could also be used to improve the crop yield of specific crops (Yang et al., 2021). Moreover, the approach could not only be used as a supplement in crop planning but to predict areas prone to extreme events (Kaur et al., 2020), and serve as a proxy for designing a monitoring network for soil moisture and water table depth when combined with more detailed models (Pereira et al., 2020).

Moving forward, one interesting aspect to explore in future works could be the incorporation of the suggested approach in the setup of more detailed land surface models. The potential to quickly assess large areas and highlight areas of interest, would not only speed up the process by eliminating areas but increase the transparency of the assessment process.

5. Conclusions

This paper discusses a new approach to assessing soil moisture. We show that, under the assumption of a topography-controlled and uniform distribution of groundwater storage, and a flat-water table, the combination of hypsometric curves and normalized terrain data it is possible to assess not only the fraction of wet areas within an area but areas of interest from a land-use perspective. In addition, by allowing the user to adjust the parameters for spatial delineation and root depth used within the assessment, the proposed approach allows for a wider application. By providing managers and researchers with a viable, quick, and cost-efficient tool to assess and identify wet areas, we believe this approach could help in the future management of water resources, including the improvement of water balance calculations and management of flood prone areas.

Conflict of Interest

The authors declare no conflicts of interest relevant to this study.

Data Availability Statement

The data and scripts associated with this study are available in the Zenodo repository at: https://doi.org/10.5281/zenodo.10470069; Bjerkén et al. (2024).

References

Ågren, A. M., Larson, J., Paul, S. S., Laudon, H., & Lidberg, W. (2021). Use of multiple LIDAR-derived digital terrain indices and machine learning for high-resolution national-scale soil moisture mapping of the Swedish forest landscape. *Geoderma*, *404*, 115280. https://doi.org/10.1016/j.geoderma.2021.115280

Alvarenga, L. A., Mello, C. R. d., Colombo, A., & Cuartas, L. A. (2017). Performance of a distributed hydrological model based on soil and moisture zone maps. *Revista Brasileira de Ciência do Solo*, *41*(0). https://doi.org/10.1590/18069657rbcs20160551

Atkinson, S., Woods, R., & Sivapalan, M. (2002). Climate and landscape controls on water balance model complexity over changing timescales. *Water Resources Research*, *38*(12), 50-51–50-17. https://doi.org/10.1029/2002WR001487

Babaeian, E., Paheding, S., Siddique, N., Devabhaktuni, V. K., & Tuller, M. (2021). Estimation of root zone soil moisture from ground and remotely sensed soil information with multisensor data fusion and automated machine learning. *Remote Sensing of Environment*, *260*, 112434. https://doi.org/10.1016/j.rse.2021.112434

Barling, R. D., Moore, I. D., & Grayson, R. B. (1994). A quasi-dynamic wetness index for characterizing the spatial distribution of zones of surface saturation and soil water content. *Water Resources Research*, *30*(4), 1029–1044. https://doi.org/10.1029/93WR03346

Bartsch, A., Balzter, H., & George, C. (2009). The influence of regional surface soil moisture anomalies on forest fires in Siberia observed from satellites. *Environmental Research Letters*, *4*(4), 045021. https://doi.org/10.1088/1748-9326/4/4/045021

Beck, H. E., Zimmermann, N. E., McVicar, T. R., Vergopolan, N., Berg, A., & Wood, E. F. (2018). Present and future Köppen-Geiger climate classification maps at 1-km resolution. *Scientific Data*, *5*(1), 1–12. https://doi.org/10.1038/sdata.2018.214

Bittelli, M. (2011). Measuring soil water content: A review. *HortTechnology*, *21*(3), 293–300. https://doi.org/10.21273/HORTTECH.21.3.293

Bjerkén, A., Cuartes, L. A., Peeters, L., & Persson, K. M. (2024). Spatial data, modelling software and associated scripts for the assessment of surface saturation and transpiration potential. [Dataset]. *Zenodo*. https://doi.org/10.5281/zenodo.10470069

Bjerkén, A., & Persson, K. M. (2021). Evaluating GIS based water budget components applicability and availability for the Lagan River catchment. *Vatten: tidskrift för vattenvård/Journal of Water Management and research*, *77*(4), 229–238. Retrieved from https://www.tidskriftenvatten.se/wp-content/uploads/2021/12/21202_nr-4_229-238.pdf

Bolten, J., & Crow, W. (2012). Improved prediction of quasi-global vegetation conditions using remotely-sensed surface soil moisture. *Geophysical Research Letters*, *39*(19). https://doi.org/10.1029/2012GL053470

Brocca, L., Melone, F., Moramarco, T., Wagner, W., & Hasenauer, S. (2010). ASCAT soil wetness index validation through in situ and modeled soil moisture data in central Italy. *Remote Sensing of Environment*, *114*(11), 2745–2755. https://doi.org/10.1016/j.rse.2010.06.009

Brocca, L., Tullo, T., Melone, F., Moramarco, T., & Morbidelli, R. (2012). Catchment scale soil moisture spatial–temporal variability. *Journal of Hydrology*, *422*, 63–75. https://doi.org/10.1016/j.jhydrol.2011.12.039

Canadell, J., Jackson, R., Ehleringer, J., Mooney, H., Sala, O., & Schulze, E.-D. (1996). Maximum rooting depth of vegetation types at the global scale. *Oecologia*, *108*(4), 583–595. https://doi.org/10.1007/BF00329030

Capehart, W. J., & Carlson, T. N. (1997). Decoupling of surface and near-surface soil water content: A remote sensing perspective. *Water Resources Research*, *33*(6), 1383–1395. https://doi.org/10.1029/97WR00617

Chaney, N. W., Roundy, J. K., Herrera-Estrada, J. E., & Wood, E. F. (2015). High-resolution modeling of the spatial heterogeneity of soil moisture: Applications in network design. *Water Resources Research*, *51*(1), 619–638. https://doi.org/10.1002/2013WR014964

Condon, L. E., Atchley, A. L., & Maxwell, R. M. (2020). Evapotranspiration depletes groundwater under warming over the contiguous United States. *Nature Communications*, *11*(1), 873. https://doi.org/10.1038/s41467-020-14688-0

Condon, L. E., & Maxwell, R. M. (2015). Evaluating the relationship between topography and groundwater using outputs from a continental-scale integrated hydrology model. *Water Resources Research*, *51*(8), 6602–6621. https://doi.org/10.1002/2014WR016774

Cuartas, L. A., Tomasella, J., Nobre, A. D., Nobre, C. A., Hodnett, M. G., de Oliveira, S. M., et al. (2012). Distributed hydrological modeling of a micro-scale rainforest watershed in Amazonia: Model evaluation and advances in calibration using the new HAND terrain model. *Journal of Hydrology*, *462*, 15–27. https://doi.org/10.1016/j.jhydrol.2011.12.047

Dobriyal, P., Qureshi, A., Badola, R., & Hussain, S. A. (2012). A review of the methods available for estimating soil moisture and its implications for water resource management. *Journal of Hydrology*, *458*, 110–117. https://doi.org/10.1016/j.jhydrol.2012.06.021

Dorigo, W., Wagner, W., Albergel, C., Albrecht, F., Balsamo, G., Brocca, L., et al. (2017). ESA CCI Soil Moisture for improved Earth system understanding: State-of-the art and future directions. *Remote Sensing of Environment*, *203*, 185–215. https://doi.org/10.1016/j.rse.2017.07.001

Durrant, M., Love, B., Messem, A., & Draycott, A. (1973). Growth of crop roots in relation to soil moisture extraction. *Annals of Applied Biology*, *74*(3), 387–394. https://doi.org/10.1111/j.1744-7348.1973.tb07759.x

Evett, S. R., Schwartz, R. C., Casanova, J. J., & Heng, L. K. (2012). Soil water sensing for water balance, ET and WUE. *Agricultural Water Management*, *104*, 1–9. https://doi.org/10.1016/j.agwat.2011.12.002

Fang, L., Zhang, Z., & Huang, J. (2023). Rapid flood modelling using HAND-FFA-SRC coupled approach and social media-based geodata in a coastal Chinese watershed. *Environmental Modelling & Software*, *170*, 105862. https://doi.org/10.1016/j.envsoft.2023.105862

Gharari, S., Hrachowitz, M., Fenicia, F., & Savenije, H. (2011). Hydrological landscape classification: Investigating the performance of HAND based landscape classifications in a central European meso-scale catchment. *Hydrology and Earth System Sciences*, *15*(11), 3275–3291. https://doi.org/10.5194/hess-15-3275-2011

Gleeson, T., Marklund, L., Smith, L., & Manning, A. H. (2011). Classifying the water table at regional to continental scales. *Geophysical Research Letters*, *38*(5). https://doi.org/10.1029/2010GL046427

Grabs, T., Seibert, J., Bishop, K., & Laudon, H. (2009). Modeling spatial patterns of saturated areas: A comparison of the topographic wetness index and a dynamic distributed model. *Journal of Hydrology*, *373*(1–2), 15–23. https://doi.org/10.1016/j.jhydrol.2009.03.031

Haitjema, H. M., & Mitchell-Bruker, S. (2005). Are water tables a subdued replica of the topography? *Ground Water*, *43*(6), 781–786. https://doi.org/10.1111/j.1745-6584.2005.00090.x

Hashemian, M., Ryu, D., Crow, W. T., & Kustas, W. P. (2015). Improving root-zone soil moisture estimations using dynamic root growth and crop phenology. *Advances in Water Resources*, *86*, 170–183. https://doi.org/10.1016/j.advwatres.2015.10.001

Heathman, G. C., Starks, P. J., Ahuja, L. R., & Jackson, T. J. (2003). Assimilation of surface soil moisture to estimate profile soil water content. *Journal of Hydrology*, *279*(1–4), 1–17. https://doi.org/10.1016/S0022-1694(03)00088-X

Huisman, J. A., Hubbard, S. S., Redman, J. D., & Annan, A. P. (2003). Measuring soil water content with ground penetrating radar: A review. *Vadose Zone Journal*, *2*(4), 476–491. https://doi.org/10.2113/2.4.476

Johnston, R., & Smakhtin, V. (2014). Hydrological modeling of large river basins: How much is enough? *Water Resources Management*, *28*(10), 2695–2730. https://doi.org/10.1007/s11269-014-0637-8

Kaufmann, M. S., Klotzsche, A., Vereecken, H., & van der Kruk, J. (2020). Simultaneous multichannel multi-offset ground-penetrating radar measurements for soil characterization. *Vadose Zone Journal*, *19*(1), e20017. https://doi.org/10.1002/vzj2.20017

Kaur, G., Singh, G., Motavalli, P. P., Nelson, K. A., Orlowski, J. M., & Golden, B. R. (2020). Impacts and management strategies for crop production in waterlogged or flooded soils: A review. *Agronomy Journal*, *112*(3), 1475–1501. https://doi.org/10.1002/agj2.20093

Keetch, J. J., & Byram, G. M. (1968). *A drought index for forest fire control* (Vol. 38). US Department of Agriculture, Forest Service.

Klante, C., Larson, M., & Persson, K. M. (2021). Brownification in Lake Bolmen, Sweden, and its relationship to natural and human-induced changes. *Journal of Hydrology: Regional Studies*, *36*, 100863. https://doi.org/10.1016/j.ejrh.2021.100863

Klotzsche, A., Jonard, F., Looms, M. C., van der Kruk, J., & Huisman, J. A. (2018). Measuring soil water content with ground penetrating radar: A decade of progress. *Vadose Zone Journal*, *17*(1), 1–9. https://doi.org/10.2136/vzj2018.03.0052

Komolafe, A., Awe, B., Olorunfemi, I., & Oguntunde, P. (2020). Modelling flood-prone area and vulnerability using integration of multi-criteria analysis and HAND model in the Ogun River Basin, Nigeria. *Hydrological Sciences Journal*, *65*(10), 1766–1783. https://doi.org/10.1080/02626667.2020.1764960

Korres, W., Reichenau, T., Fiener, P., Koyama, C., Bogena, H. R., Cornelissen, T., et al. (2015). Spatio-temporal soil moisture patterns–A meta-analysis using plot to catchment scale data. *Journal of Hydrology*, *520*, 326–341. https://doi.org/10.1016/j.jhydrol.2014.11.042

Langbein, W. B. (1947). Topographic characteristics of drainage basins. Retrieved from https://pubs.usgs.gov/wsp/0968c/report.pdf

Legates, D. R., Mahmood, R., Levia, D. F., DeLiberty, T. L., Quiring, S. M., Houser, C., & Nelson, F. E. (2011). Soil moisture: A central and unifying theme in physical geography. *Progress in Physical Geography*, *35*(1), 65–86. https://doi.org/10.1177/0309133310386514

Liu, J., Yang, H., Gosling, S. N., Kummu, M., Flörke, M., Pfister, S., et al. (2017). Water scarcity assessments in the past, present, and future. *Earth's Future*, *5*(6), 545–559. https://doi.org/10.1002/2016EF000518

Meng, L., & Quiring, S. M. (2008). A comparison of soil moisture models using soil climate analysis network observations. *Journal of Hydrometeorology*, *9*(4), 641–659. https://doi.org/10.1175/2008JHM916.1

Neale, C. M., Geli, H. M., Kustas, W. P., Alfieri, J. G., Gowda, P. H., Evett, S. R., et al. (2012). Soil water content estimation using a remote sensing based hybrid evapotranspiration modeling approach. *Advances in Water Resources*, *50*, 152–161. https://doi.org/10.1016/j.advwatres.2012.10.008

Nobre, A. D., Cuartas, L. A., Hodnett, M., Rennó, C. D., Rodrigues, G., Silveira, A., & Saleska, S. (2011). Height above the Nearest Drainage–a hydrologically relevant new terrain model. *Journal of Hydrology*, *404*(1–2), 13–29. https://doi.org/10.1016/j.jhydrol.2011.03.051

Nobre, A. D., Cuartas, L. A., Momo, M. R., Severo, D. L., Pinheiro, A., & Nobre, C. A. (2016). HAND contour: A new proxy predictor of inundation extent. *Hydrological Processes*, *30*(2), 320–333. https://doi.org/10.1002/hyp.10581

Peeters, L., Crosbie, R., & Van Dijk, A. (2011). *Incorporating groundwater dynamics and clay content in AWRA-L (A water information R & D alliance between the Bureau of Meteorology and CSIRO's Water for a Healthy Country Flagship*. CSIRO.

Peeters, L., Crosbie, R. S., Doble, R. C., & Van Dijk, A. I. (2013). Conceptual evaluation of continental land-surface model behaviour. *Environmental Modelling & Software*, *43*, 49–59. https://doi.org/10.1016/j.envsoft.2013.01.007

Pereira, L., Paredes, P., & Jovanovic, N. (2020). Soil water balance models for determining crop water and irrigation requirements and irrigation scheduling focusing on the FAO56 method and the dual Kc approach. *Agricultural Water Management*, *241*, 106357. https://doi.org/10.1016/j.agwat.2020.106357

Rakhmatulina, E., Stephens, S., & Thompson, S. (2021). Soil moisture influences on Sierra Nevada dead fuel moisture content and fire risks. *Forest Ecology and Management*, *496*, 119379. https://doi.org/10.1016/j.foreco.2021.119379

Renzullo, L. J., Van Dijk, A., Perraud, J.-M., Collins, D., Henderson, B., Jin, H., et al. (2014). Continental satellite soil moisture data assimilation improves root-zone moisture analysis for water resources assessment. *Journal of Hydrology*, *519*, 2747–2762. https://doi.org/10.1016/j.jhydrol.2014.08.008

Rödiger, T., Geyer, S., Mallast, U., Merz, R., Krause, P., Fischer, C., & Siebert, C. (2014). Multi-response calibration of a conceptual hydrological model in the semiarid catchment of Wadi al Arab, Jordan. *Journal of Hydrology*, *509*, 193–206. https://doi.org/10.1016/j.jhydrol.2013.11.026

Rosenbaum, U., Bogena, H. R., Herbst, M., Huisman, J. A., Peterson, T. J., Weuthen, A., et al. (2012). Seasonal and event dynamics of spatial soil moisture patterns at the small catchment scale. *Water Resources Research*, *48*(10). https://doi.org/10.1029/2011WR011518

Scriven, B. W. G., McGrath, H., & Stefanakis, E. (2021). GIS derived synthetic rating curves and HAND model to support on-the-fly flood mapping. *Natural Hazards*, *109*(2), 1629–1653. https://doi.org/10.1007/s11069-021-04892-6

Strahler, A. N. (1952). Hypsometric (area-altitude) analysis of erosional topography. *Geological Society of America Bulletin*, *63*(11), 1117–1142. https://doi.org/10.1130/0016-7606(1952)63[1117:HAAOET]2.0.CO;2

Sydvatten. (2015). Bolmen. Retrieved from https://sydvatten.se/var-verksamhet/rapporter-om-ravattentakter/bolmen-3/

Taylor, R. G., Scanlon, B., Döll, P., Rodell, M., Van Beek, R., Wada, Y., et al. (2013). Ground water and climate change. *Nature Climate Change*, *3*(4), 322–329. https://doi.org/10.1038/nclimate1744

Teuling, A. J., & Troch, P. A. (2005). Improved understanding of soil moisture variability dynamics. *Geophysical Research Letters*, *32*(5). https://doi.org/10.1029/2004GL021935

Tian, S., Tregoning, P., Renzullo, L. J., van Dijk, A. I., Walker, J. P., Pauwels, V. R., & Allgeyer, S. (2017). Improved water balance component estimates through joint assimilation of GRACE water storage and SMOS soil moisture retrievals. *Water Resources Research*, *53*(3), 1820–1840. https://doi.org/10.1002/2016WR019641

Vereecken, H., Huisman, J., Bogena, H., Vanderborght, J., Vrugt, J., & Hopmans, J. (2008). On the value of soil moisture measurements in vadose zone hydrology: A review. *Water Resources Research*, *44*(4). https://doi.org/10.1029/2008WR006829

Vivoni, E. R., Di Benedetto, F., Grimaldi, S., & Eltahir, E. A. (2008). Hypsometric control on surface and subsurface runoff. *Water Resources Research*, *44*(12). https://doi.org/10.1029/2008wr006931

Wall, D. H., & Virginia, R. A. (1999). Controls on soil biodiversity: Insights from extreme environments. *Applied Soil Ecology*, *13*(2), 137–150. https://doi.org/10.1016/S0929-1393(99)00029-3

Western, A. W., & Blöschl, G. (1999). On the spatial scaling of soil moisture. *Journal of Hydrology*, *217*(3–4), 203–224. https://doi.org/10.1016/S0022-1694(98)00232-7

Western, A. W., Grayson, R. B., & Blöschl, G. (2002). Scaling of soil moisture: A hydrologic perspective. *Annual Review of Earth and Planetary Sciences*, *30*(1), 149–180. https://doi.org/10.1146/annurev.earth.30.091201.140434

Western, A. W., Zhou, S.-L., Grayson, R. B., McMahon, T. A., Blöschl, G., & Wilson, D. J. (2004). Spatial correlation of soil moisture in small catchments and its relationship to dominant spatial hydrological processes. *Journal of Hydrology*, *286*(1–4), 113–134. https://doi.org/10.1016/j.jhydrol.2003.09.014

Wu, W.-Y., Lo, M.-H., Wada, Y., Famiglietti, J. S., Reager, J. T., Yeh, P. J.-F., et al. (2020). Divergent effects of climate change on future groundwater availability in key mid-latitude aquifers. *Nature Communications*, *11*(1), 3710. https://doi.org/10.1038/s41467-020-17581-y

Yang, M., Wang, G., Lazin, R., Shen, X., & Anagnostou, E. (2021). Impact of planting time soil moisture on cereal crop yield in the upper blue nile basin: A novel insight towards agricultural water management. *Agricultural Water Management*, *243*, 106430. https://doi.org/10.1016/j.agwat.2020.106430

Yuan, Q., Xu, H., Li, T., Shen, H., & Zhang, L. (2020). Estimating surface soil moisture from satellite observations using a generalized regression neural network trained on sparse ground-based measurements in the continental US. *Journal of Hydrology*, *580*, 124351. https://doi.org/10.1016/j.jhydrol.2019.124351

Zhou, S., Williams, A. P., Lintner, B. R., Berg, A. M., Zhang, Y., Keenan, T. F., et al. (2021). Soil moisture–atmosphere feedbacks mitigate declining water availability in drylands. *Nature Climate Change*, *11*(1), 38–44. https://doi.org/10.1038/s41558-020-00945-z